Using Implantable Artificial Dermis-PELNAC as a Functional Material to Guide Reconstruction of Finger Body Defect

Ann. Ital. Chir., 2025 96, 12: 1682–1695
https://doi.org/10.62713/aic.3871

Hu Yang[1,†], Weijie Zhou[2,†], Yanzhao Dong[1], Haiying Zhou[1], Ahmad Alhaskawi[1], Weihua Shen[3], Sohaib Hasan Abdullah Ezzi[4], Vishnu Goutham Kota[4], Mohamed Hasan Abdulla Hasan Abdulla[4], Siyi Chen[5], Feng Wen[6], Zhenyu Sun[1], Olga Alenikova[7], Sahar Ahmed Abdalbary[8], Hui Lu[1]

[1]Department of Orthopedics, The First Affiliated Hospital, Zhejiang University, 310003 Hangzhou, Zhejiang, China
[2]Department of Orthopedics, No. 903 Hospital of PLA Joint Logistic Support Force, 310003 Hangzhou, Zhejiang, China
[3]Department of Orthopedics, People's Hospital of Jingning She Autonomous County, 323500 Lishui, Zhejiang, China
[4]Zhejiang University School of Medicine, 310058 Hangzhou, Zhejiang, China
[5]Zhejiang Top-medical Medical Dressing Co., Ltd., 325600 Wenzhou, Zhejiang, China
[6]Zhejiang Engineering Research Center for Tissue Repair Materials, Wenzhou Institute, University of Chinese Academy of Sciences, 325001 Wenzhou, Zhejiang, China
[7]Department of Neurology, Republican Research and Clinical Center of Neurology and Neurosurgery, 220114 Minsk, Belarus
[8]Department of Orthopedic Physical Therapy, Faculty of Physical Therapy, Nahda University in Beni Suef, 62511 Beni Suef, Egypt

AIM: Managing partial defects of the finger is crucial for both function and aesthetics, especially when bone or tendon is exposed. Permacol Enhanced Layer for Neodermis and Coverage (PELNAC), an artificial dermis, serves as a promising scaffold in surgical procedures, providing wound protection and promoting tissue healing. This study assesses the effectiveness of PELNAC in treating a range of partial finger defects.

METHODS: We assessed PELNAC's morphology and microstructure using scanning electron microscopy, characterized its degradation profile over six weeks in simulated body fluid, and confirmed its cytocompatibility with L929 cell cultures. In the clinical setting, 47 patients with 56 partial finger defects (both superficial and deep) were treated using PELNAC alone. Outcome measures included wound closure time, range of motion (ROM), sensory recovery (two-point discrimination), Vancouver Scar Scale (VSS) scores, and patient satisfaction.

RESULTS: Scanning electron microscopy revealed interconnected micropores in PELNAC, with a porosity of 81.3 $\pm$ 2.1% and aperture sizes of 40–70 µm (top view) and 60–100 µm (section view). After six weeks in simulated body fluid, PELNAC retained 86.4 $\pm$ 1.5% of its weight, and cells proliferated well on its surface. All treated wounds healed without the need for split-thickness skin grafts, with an average closure time of 58.7 $\pm$ 12.8 days (range: 30–84 days). Age showed weak positive correlation with healing time ($r = 0.152$, $p < 0.01$) and weak negative correlation with two-point discrimination ($r = –0.55$, $p < 0.01$). Longer healing times correlated with reduced ROM ($r = –0.143$, $p < 0.01$), while higher VSS scores were linked to poorer functional outcomes ($r = –0.22$, $p < 0.01$). The average ROM in patients with distal interphalangeal joint (DIPJ) defects was 49° (IQR: 45–56.25°). Sensory recovery averaged 5.95 mm (IQR: 5.175–6.7 mm). The mean VSS score was 2 (IQR: 1–3), indicating minimal scarring. Patient satisfaction was high (functional score: 9 (IQR: 8–9.25)), with no severe complications reported.

CONCLUSIONS: This study evaluates the clinical and biomechanical effectiveness of PELNAC as a single-stage reconstructive material for partial finger defects. PELNAC facilitates wound healing without secondary skin grafts, preserving joint mobility, promoting sensory recovery, and minimizing scarring. The results highlight PELNAC as a simple, safe, and effective alternative to traditional approaches, reducing donor site morbidity and eliminating the need for multiple surgeries.

Keywords: artificial dermis; PELNAC; finger body defect; tissue regeneration

Introduction

Traumatic partial defect of the finger body frequently occurred in orthopedics and emergency. Traumatic partial defects of the finger body are often associated with various types of injuries, including cuts, blasts, avulsions, or crashes. The damage often affects the segmental mid-proximal digit, palmar distal digit, dorsal distal digit, and lateral distal digit [1]. The defect of these cases usually involves skin, nail bed, or soft tissue, with or without underlying exposure of bone or tendon.

Treating such injuries involves resurfacing the injured finger with a high-quality, sensitive skin covering while maintaining its range of motion (ROM). Management of skin and soft-tissue defects of the finger body is essential, especially when bone or tendon is exposed. Simple amputa-

Submitted: 18 November 2024 Revised: 14 March 2025 Accepted: 24 March 2025 Published: 3 December 2025
Correspondence to: Hui Lu, Department of Orthopedics, The First Affiliated Hospital, Zhejiang University, 310003 Hangzhou, Zhejiang, China (e-mail: huilu@zju.edu.cn).
[†]*These authors contributed equally.*

tion will compromise the finger's look and function in situations of traumatic defect of finger segments. The traditional reconstructive operations include free skin transplantation, V-Y type advanced flap (a triangular flap technique), cross-finger flap, thenar pedicle flap, abdominal pedicle flap, reverse digital artery island flap, and free flap. Free skin transplantation is not applicable when bone or tendon is exposed. Even though flap surgery can keep a finger's length intact, the majority of the reconstructed finger lacks a skin crease or fingernail, and feeling recovery is hindered. Each of these methods has clear drawbacks of its own [2].

Bioengineered skin replacements are an appealing option to other therapies that physicians might utilize. Acting as a matrix, the artificial dermis covers the wound and aids in tissue regeneration and repair. Collagen and elastin are examples of the extracellular and cellular components that make up the bioengineered and biocompatible polymer matrix used in its products. In 1981, in order to cure severe burn injuries, Yannas *et al*. [3] and Burke *et al*. [4] created the first "modern" artificial dermal replacement. Since then, many types of artificial dermis goods, such as Dermagraft, Terudermis [5], Matriderm, and Permacol Enhanced Layer for Neodermis and Coverage (PELNAC) [6] have been put on the market and become a popular option in reconstructive surgical sectors. Many studies have looked at the application of dermal replacements in reconstructive surgery. These products are primarily used to treat burns, ulcers, and chronic wounds in an effort to replicate the mechanical characteristics of healthy skin and prevent toxicity or immunological reactions [7,8]. Multiple healing mechanisms, including localized inflammation; infiltration of neutrophils, macrophages polarization, fibroblasts proliferation, and keratinocytes migration; and neovascularization of the scaffold during recovery [9]. PELNAC is a common artificial dermis. It has a deep layer constituted by a porcine origin 3-dimensional collagen matrix which could integrate into the defect and prompt cellular behaviors such as migration, proliferation, and differentiation. It will also provide interconnective proses and proper elasticity. The superficial layer made by a silicon sheet serving as a temporary artificial epidermis against dehydration, microorganisms, and toxins [10]. There are two steps in the typical PELNAC application process. First, the dermal matrix covers the lesion. A few weeks later, the silicon layer is removed, and an autologous split or full-thickness skin transplant is applied. Remarkably, a number of studies have demonstrated that utilizing artificial dermis alone was sufficient to induce one-stage wound healing of scalp and face abnormalities (range: 1.3–63.5 cm^2) [11–13]. This study uniquely evaluates PELNAC as a standalone material for both superficial and deep finger defects, challenging the conventional two-stage approach.

Materials and Methods

Materials

Artificial dermal substitute-PELNAC was purchased from Gunze Corp, Osaka, Japan. Simulated body fluid (SBF) was bought from Leagene Biotechnology, Beijing, China. L929 cells were purchased from National Collection of Authenticated Cell Cultures, China. Cells were STR identified and mycoplasma free. Thermo Fisher supplied the penicillin-streptomycin, fetal bovine serum (FBS), and Dulbecco's modified Eagle's medium (DMEM) medium (high glucose). Every other chemical was analytical grade and was put to work right away.

Material Characterization

Surface Morphology and Microstructure

Scanning electron microscope (SEM, Phenom Pharos, Thermo Fisher Scientific, Eindhoven, Holland) with an acceleration voltage of 15 kV was used to observe the morphology and microstructure of PELNAC. A platinum ion coater was used to coat the samples for 120 seconds at 10 mA (EM, ACE600, Leica, Germany) and analyzed using SEM equipment. The pore diameters and distributions were analyzed using ImageJ (1.40G, National Institutes of Health, Bethesda, MD, USA) [14]. Beside SEM experiments, the porosity and liquid absorbency of PELNAC were measured as well according to previous reports [15,16].

Degradation

In vitro degradation test was conducted according to previous study with some modifications [17]. PELNAC was sectioned into 1 cm × 1 cm pieces, lyophilized, and precisely measured before being placed in sterile centrifuge tubes with 5 mL of SBF. The sealed tubes were maintained at 37 °C for periods ranging from 1 to 6 weeks. At designated intervals, the specimens were removed, cleaned with Deionized (DI) water, freeze-dried again, and their mass recorded. The mass loss of the samples was determined using the following formula: weight loss (%) = $(W_0 - W_t)/W_0 \times 100$, where W_0 represents the initial weight (g) of the dried sample before incubation and W_t represents the weight of the degraded sample after the respective time points.

Cell Experiments

Cell Culture

High glucose Dulbecco's modified Eagle's medium (DMEM) supplemented with 10% fetal bovine serum and a 1% penicillin mixture was used to culture L929 cells. The culture medium was replaced every 2–3 days. Cells were cultured until they reached 80–90% confluence. Subsequently, Trypsin- Ethylenediaminetetraacetic Acid (Trypsin-EDTA) was employed to detach the cells from the tissue flask bottles, which were then transferred to a new Petri dish. For further experimentation, cells from passages 2 to 5 were utilized. Throughout the subculturing

process, all cells were maintained in a constant temperature incubator set at 37 °C with 5% CO_2.

Cytocompatibility

Cytocompatibility of PELNAC was evaluated through cell adhesion and proliferation on its surface according to previous study [15]. Cell seeding was conducted at a density of 5×10^5 cells per PELNAC samples, with cell-free samples used as control for all the following work. Cells in PELNAC were incubated for 7 days. Cell attachment and proliferation of L929 cultivated in PELNAC samples was assessed by SEM. The samples were fixed with 2.5 wt % glutaraldehyde in Phosphate buffered saline (PBS) for one hour at room temperature in order to observe them using a SEM. They were then dehydrated sequentially with ethanol series (25, 50, 75, 95, and 100% (v/v) 15 min each) and hexamethyldisilazane for 15 min, and finally air dried at ambient temperature. Samples were examined using a SEM after being coated with a platinum ion coater for 120 seconds at 10 mA.

Methods

From June 2014 to August 2019, a series of 47 patients with partial finger body defects were treated with PELNAC in the First Affiliated Hospital (Zhejiang University) including, 15 women have 17 digits, while 32 males have 39. They were between 15 and 70 years old.

The Inclusion Criteria

(1) Traumatic partial finger defects (superficial or deep) with exposed underlying tissue (soft tissue, tendon, or bone).
(2) Age between 15 and 70 years.
(3) Absence of pre-existing conditions affecting wound healing (e.g., peripheral vascular disease, immunodeficiency).

The Exclusion Criteria

(1) Advanced age: Patients aged 70 years or older were excluded.
(2) Diabetes: Patients with diabetes were excluded due to potential complications in wound healing.
(3) Heavy smoking: Patients who were heavy smokers were excluded, as smoking can impair wound healing.
(4) Long-term Use of Glucocorticoids: Patients who had a history of long-term use of glucocorticoids were excluded, as these medications can affect the healing process.
The source of patients included: (i) 20 fingers with twist injury, (ii) 10 fingers with a sharp cut, and (iii) 14 fingers with crash injury, (iv) 12 fingers with an electric saw injury. The depth of the wound was superficial in 29 (61.7%) patients, and deep (with tendon or bone exposure) in 18 (38.3%) patients.
Before employing PELNAC for coverage, the author of this study explained all potential treatment options to each patient, including V-Y advancement flap, autologous skin graft, artificial dermis graft, pedicle flap, reverse digital artery island flap, and free flap transplantation.
The procedure was performed under brachial plexus block anesthesia or digital nerve block anesthesia. Following thorough debridement and hemostasis, the wound was covered with PELNAC according to the manufacturer's instructions. Initially, the PELNAC was customized to match the shape and size of the defect. It was then soaked in saline for 15 seconds prior to application. Next, the PELNAC was secured to the defect using 4/0 Prolene sutures. Additionally, small drainage holes were created in the silicon film. All surgeries were conducted by the same surgeon. Dressings were changed every 2–3 days, and the wound was maintained in a moist environment until complete reepithelialization occurred. The silicon film remained in place until the wound was fully healed.
Efficacy was determined using objective and subjective measures. The objective effectiveness criteria were: (1) time for total wound closure, (2) sensory recovery (static two-point discrimination test), (3) ROM, and (4) scar quality (Vancouver Scar Scale, VSS) [18]. The static two-point discrimination was measured at the end of the follow-up period.
The subjective efficacy criteria were: (1) patient's level of satisfaction at 12 months postoperatively using a visual analog scale (VAS, 0 = the worst and 10 = the best) [19]; (2) patient's tactile sense of the treated area at 12 months postoperatively (normal, nearly normal, mild numbness, and severe numbness).

Statistical Analysis

The SPSS for Windows, version 22.0 (IBM Corp., Armonk, NY, USA) was used to enter and analyze the data. In statistical analysis, continuous variables (such as age, healing time) will be described using mean ± standard deviation (SD). If the data are not normally distributed, median and interquartile range (IQR) will be used. The normality of continuous variables will be assessed using the Shapiro-Wilk test. Categorical variables (such as gender, injury type, and defect depth) will be presented as frequencies and percentages. For group comparisons, normally distributed continuous variables will be analyzed using independent *t*-tests or one-way analysis of variance (ANOVA). If ANOVA shows significant differences, post-hoc analysis using Tukey's test will be performed to identify specific group differences. For continuous variables that do not follow a normal distribution, Mann-Whitney U tests or Kruskal-Wallis tests will be used for group comparisons.
The data for ROM and two-point discrimination do not follow a normal distribution. Correlation analysis will be performed using Spearman's rank correlation coefficient to assess the relationships between continuous variables. The correlation coefficient (r) and *p*-values will be reported to assess the significance of the correlations, with *p*-values less than 0.05 considered statistically significant.

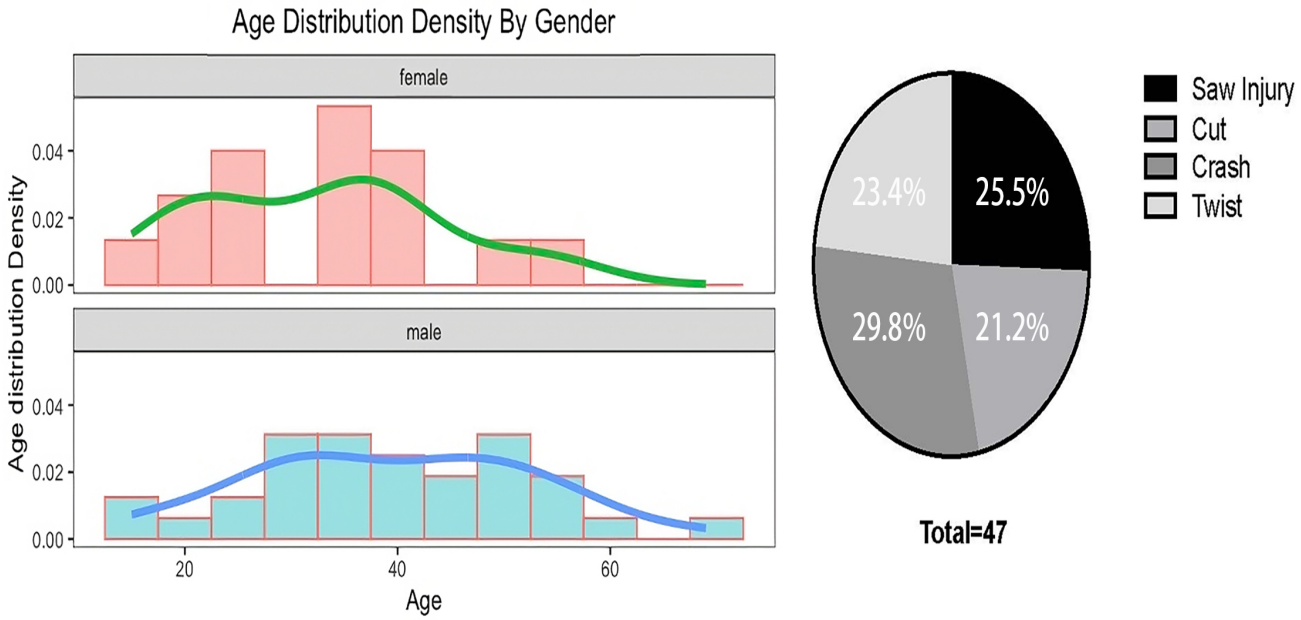

Fig. 1. Age distribution and injury etiology of the cohort. (Left) Age distribution of patients, stratified by gender (male vs. female). (Right) Distribution of injury etiologies, categorized into four types: twist injury, sharp cut, crash injury, and electric saw injury. Percentages reflect the proportion of each injury type within the cohort.

All statistical analyses will be conducted using two-tailed tests, with *p*-values less than 0.05 indicating statistical significance. *p*-values and correlation coefficients will be reported in the results section, with all data analyzed using appropriate statistical software.

Results

We studied the clinical efficacy of using artificial dermis solely for one-stage wound healing in all kinds of partial finger body defects (with or without bone/tendon exposure). All the cases healed well without a second-stage skin graft (Table 1).

Clinical Treatment

A total of 47 patients (56 digits) were included in this study (Fig. 1), which illustrates the cohort's age distribution (stratified by gender) and injury etiology proportions (twist injury, sharp cut, crash injury, and electric saw injury) and all of them had a follow-up time of 12-18 months. Finger body defects of 21 digits were superficial without tendon or bone exposure. Finger body defects of 7 digits were deep with tendon exposure, and 10 digits were deep with bone exposure. All the patients healed well with good quality and esthetic contours. No signs of complications such as infection, hematoma formation, seroma formation or painful scar were observed. None of them required additional operation.

Demographic analysis (Table 2) revealed no significant difference in age between male (mean 39.6 $\pm$ 13.1 years) and female patients (mean 32.9 $\pm$ 11.3 years, $p = 0.426$). Healing times differed significantly among injury types (ANOVA $p < 0.001$), with cut injuries demonstrating the shortest healing duration (42.9 $\pm$ 6.62 days), significantly faster than crash (63.8 $\pm$ 7.47 days), saw (61.5 $\pm$ 13.5 days), and twist injuries (62 $\pm$ 10.94 days; post-hoc $p < 0.01$). Age showed weak positive correlations with healing time ($r = 0.152$, $p < 0.01$) and negative correlations with two-point discrimination ($r = –0.55$, $p < 0.01$). Longer healing times were associated with reduced ROM ($r = –0.143$, $p < 0.01$). The time to re-epithelialization of the wound was 58.7 $\pm$ 12.8 days on average (range, 30–84 days). The median superficial defects healed in 48.5 (IQR: 42.5–55.25 days), while median deep defects required 65.5 (IQR: 59.75–70.25 days) for full wound healing. The median two-point discrimination was 5.95 mm (IQR: 5.175–6.7 mm), and a small area of finger body defect healed with smaller two-point discrimination than a large area of finger body defect. The mean two-point discrimination values varied by finger: thumb 5.75 mm (IQR: 5.4–5.875 mm), index 5.9 mm (IQR: 5.1–6.6 mm), middle 5.65 mm (IQR: 5.15–6.2 mm), ring 6.6 mm (IQR: 6.425–6.925 mm), and little 6.1 mm (IQR: 5–7.4 mm). A correlation analysis showed a weak positive correlation between age and two-point discrimination ($r = –0.55$, $p < 0.01$), suggesting that older patients may have slightly poorer sensory recovery. The median VSS was 2 (IQR: 1–3). VSS scores correlated negatively with functional scores ($r = –0.22$, $p < 0.01$), indicating that higher scar scores were associated with poorer functional outcomes. The tactile sense of the treated area at 12 months was normal in 18 patients, nearly normal in 12 patients, mild numbness in 5 patients. None of the patients suffered severe numbness. All patients were satisfied with their therapeutic outcome (The median functional score was 9 (IQR: 8–9.25)).

Table 1. Basic information of selected patients.

Sex	Age (year)	Finger	Cause	Healing time (day)	Flow-up time (day)	Rom (degrees)	Two-point discrimination (mm)	VSS	Functional score	Defect area
Male	50	Index, ring	Saw injury	37/42	12	45/63	5.2/5.9	2	9	Defect at the level of the distal interphalangeal joint.
Male	42	Ring	Cut	30	12	35	6.5	3	8	Defect at the level of the distal interphalangeal joint.
Male	69	Ring	Crash	67	18	40	7.9	4	8	Defect distal to the area from the nail root fold to the middle 1/2 of the distal interphalangeal joint.
Female	23	Index	Twist	41	16	52	5	1	8	Defect distal to the nail root fold.
Male	37	Middle	Twist	57	14	49	5.1	1	9	Defect distal to the area from the nail root fold to the Middle 1/2 of the distal interphalangeal joint.
Female	54	Middle	Cut	39	13	56	5.1	1	10	Defect at the level of the distal interphalangeal joint.
Male	56	Thumb	Saw injury	69	13	45	4.9	1	9	Defect at the level of the distal interphalangeal joint.
Female	36	Middle	Twist	60	18	50	5.4	1	10	Defect at the level of the distal interphalangeal joint.
Male	49	Index	Cut	48	12	67	5.3	1	9	Defect distal to the nail root fold.
Male	47	Middle	Crash	70	14	48	6.2	2	8	Defect at the level of the distal interphalangeal joint.
Female	24	Middle, index	Cut	45/38	12	50/59	6.1/7.0	3	10	Defect distal to the nail root fold.
Male	19	Ring	Crash	53	17	47	6.7	3	7	Defect distal to the area from the nail root fold to the middle 1/2 of the distal interphalangeal joint.
Male	45	Ring	Saw injury	63	12	37	7.4	3	10	Defect at the level of the distal interphalangeal joint.
Male	15	Middle	Crash	65	15	51	6.4	2	7	Defect at the level of the distal interphalangeal joint.
Female	36	Thumb	Crash	61	17	45	5.3	1	9	Defect distal to the area from the nail root fold to the middle 1/2 of the distal interphalangeal joint.
Male	29	Index	Cut	45	12	57	4.8	1	9	Defect distal to the nail root fold.
Male	59	Index, middle	Saw injury	53/77	17	57/50	5.9/5.5	2	10	Defect distal to the nail root fold.
Male	33	Index	Twist	39	18	68	6.7	3	10	Defect of the distal 1/2 of the nail bed.
Female	23	Index	Saw injury	59	18	43	5	1	9	Defect at the level of the distal interphalangeal joint.
Male	38	Index, middle	Crash	67/56	12	40/44	5.1/5.0	1	10	Defect at the level of the distal interphalangeal joint.
Female	17	Ring	Saw injury	71	13	50	6.5	3	9	Defect at the level of the distal interphalangeal joint.
Male	26	Thumb	Twist	75	12	47	6.8	3	9	Defect at the level of the distal interphalangeal joint.
Male	55	Ring	Saw injury	68	12	41	4.9	1	9	Defect at the level of the distal interphalangeal joint.
Male	42	Index, middle	Cut	51/38	12	65/61	6.4/6.2	2	9	Defect of the distal 1/2 of the nail bed.
Male	29	Thumb	Crash	55	13	45	5.7	2	8	Defect of the distal 1/2 of the nail bed.
Male	31	Middle	Cut	43	12	75	7.8	4	9	Defect distal to the nail root fold.
Male	42	Middle	Saw injury	75	15	48	5.1	1	10	Defect at the level of the distal interphalangeal joint.
Male	33	Little	Twist	65	14	44	4.9	1	10	Defect at the level of the distal interphalangeal joint.
Female	39	Ring, little	Crash	56/49	12	44/45	4.9/5.0	1	9	Defect of the distal 1/2 of the nail bed.
Male	25	Middle	Cut	47	14	64	7.4	4	8	Defect of the distal 1/2 of the nail bed.
Male	29	Little	Saw injury	66	12	40	7.8	4	7	Defect at the level of the distal interphalangeal joint.

Table 1. Continued.

Sex	Age (year)	Finger	Cause	Healing time (day)	Flow-up time (day)	Rom (degrees)	Two-point discrimination (mm)	VSS	Functional score	Defect area
Male	52	Index	Crash	72	16	49	6.3	2	9	Defect at the level of the distal interphalangeal joint.
Female	21	Thumb	Twist	60	14	47	5.9	1	8	Defect at the level of the distal interphalangeal joint.
Male	17	Middle, ring	Saw injury	49/62	12	65/58	5.3/6.4	2	8	Defect of the distal 1/2 of the nail bed.
Female	20	Little	Crash	56	13	46	6	2	10	Defect at the level of the distal interphalangeal joint.
Male	29	Ring, little	Crash	56/74	17	66/50	6.7/7.2	3	9	Defect of the distal 1/2 of the nail bed.
Male	57	Little	Twist	64	15	49	6.1	2	9	Defect at the level of the distal interphalangeal joint.
Male	48	Index	Saw injury	77	12	51	6.6	3	8	Defect at the level of the distal interphalangeal joint.
Male	47	Little	Cut	41	15	63	7.4	4	7	Defect of the distal 1/2 of the nail bed.
Female	39	Middle	Crash	69	17	45	5.6	1	7	Defect at the level of the distal interphalangeal joint.
Male	35	Index	Twist	61	17	39	9	5	10	Defect distal to the area from the nail root fold to the middle 1/2 of the distal interphalangeal joint.
Male	49	Ring, little	Twist	72/63	12	35/47	7.0/7.4	3	7	Defect at the level of the distal interphalangeal joint.
Female	37	Little	Saw injury	67	14	41	5	1	8	Defect at the level of the distal interphalangeal joint.
Female	34	Middle	Twist	79	18	50	6.2	2	9	Defect at the level of the distal interphalangeal joint.
Female	39	Middle	Crash	72	12	51	5.9	2	9	Defect at the level of the distal interphalangeal joint.
Female	52	Thumb	Cut	84	16	55	5.8	2	9	Defect at the level of the distal interphalangeal joint.
Male	33	Middle	Crash	67	18	49	5.7	2	8	Defect at the level of the distal interphalangeal joint.

VSS, Vancouver Scar Scale.

Table 2. Summary of study findings.

Analysis category	Variable/group	Results/values
Demographic analysis	Male patients' age	39.6 ± 13.1 years
	Female patients' age	32.9 ± 11.3 years
Healing time analysis	Injury cause (ANOVA)	Cut injury (42.9 ± 6.62 days)
		Crash injury (63.8 ± 7.47 days)
		Saw injury (61.5 ± 13.5 days)
		Twist injury (62 ± 10.94 days)
	Defect depth	Superficial defects: 48.5 (IQR: 42.5–55.25 days)
		Deep defects: 65.5 (IQR: 59.75–70.25 days)
Correlation analysis	Age vs. healing time	r = 0.152, $p < 0.01$ (weak positive correlation)
	Age vs. two-point discrimination	r = –0.55, $p < 0.01$ (negative correlation)
	Healing time vs. ROM	r = –0.143, $p < 0.01$ (negative correlation)
	VSS score vs. functional score	r = –0.22, $p < 0.01$ (negative correlation)
Functional & sensory recovery	Two-point discrimination (by fingers)	Thumb: 5.75 mm (IQR: 5.4–5.875 mm)
		Index: 5.9 mm (IQR: 5.1–6.6 mm)
		Middle: 5.65 mm (IQR: 5.15–6.2 mm)
		Ring: 6.6 mm (IQR: 6.425–6.925 mm)
		Little: 6.1 mm (IQR: 5–7.4 mm)
	ROM (DIPJ defect patients)	49° (IQR: 45–56.25°)
Scar assessment	Vancouver Scar Scale (VSS)	2 (IQR: 1–3)
	Functional score (satisfaction)	9 (IQR: 8–9.25)
Age		$p = 0.426$
Different injury causes		$p < 0.001$

ANOVA, analysis of variance; ROM, range of motion; IQR, interquartile range; DIPJ, distal interphalangeal joint.

The analysis indicates that PELNAC is effective in treating traumatic partial finger defects, with significant differences in healing times based on the cause of injury. Older patients may experience longer healing times and slightly poorer sensory recovery. Functional outcomes are influenced by age, healing time, and sensory recovery, with longer follow-up periods associated with better outcomes.

Case 1

A 50-year-old man who suffered from an electric saw injury presented with a partial lateral soft tissue defect in DIPJ of the index finger and fingertip defect of the ring finger with underlying bone exposure (Fig. 2A,B). Artificial dermis was covered on the wound after primary debridement (Fig. 2C). The wound of index finger healed at 37 days postoperatively, and the wound of the ring finger healed at 42 days postoperatively. ROM of the DIPJ of the index finger was 45 degrees, VSS score is 2, VAS score is 1, the treatment area of sensory feels good and two-point discrimination is 5.9 mm. Both wounds healed with nearly normal skin structure, a scar on the index finger was linear, and a scar on the ring finger was nearly invisible (Fig. 2D,E).

Case 2

A 42-year-old man was injured by a sharp cut, leading to a superficial skin and soft tissue defect of the fingertip in ring finger (Fig. 3A). Artificial dermis was covered on the wound after primary debridement (Fig. 3B). The wound was healed 30 days after surgery. ROM of the DIPJ of the index finger was 35 degrees, VSS score is 3, VAS score is 1, the treatment area of sensory feels good and two-point discrimination is 6.5 mm. The reborn skin was similar in color and texture to normal skin (Fig. 3C). Scar was nearly invisible.

Case 3

A 55-year-old man suffered from a crash injury during working in the factory. The injury led to a large area of deep defect in the distal phalange of ring finger with bone exposure (Fig. 4A,B). After debridement, artificial dermis was covered on the wound (Fig. 4C). The reborn tissue and skin can be seen under the silicon layer at 8 weeks postoperatively (Fig. 4D). The wound healed fully after 68 days. ROM of the DIPJ of the index finger was 41 degrees, VSS score is 1, VAS score is 2, the treatment area of sensory have a slight numbness and two-point discrimination is 4.9 mm.

Morphology and Microstructure

The morphology and microstructure of bioengineered skin substitutes are important as they will prompt not only cell behavior such as adhesion, proliferation, and infiltration into scaffolds but also facilities nutrients exchange between core of scaffold and surrounding [20]. Fig. 5 demonstrates the morphology and microstructure of artificial dermal substitute-PELNAC. It was clearly demonstrated that PELNAC possesses many interconnective pores and major pore diameters range from 40 to 70 μm analysed from top view images (Fig. 5A–C). However, the major pore di-

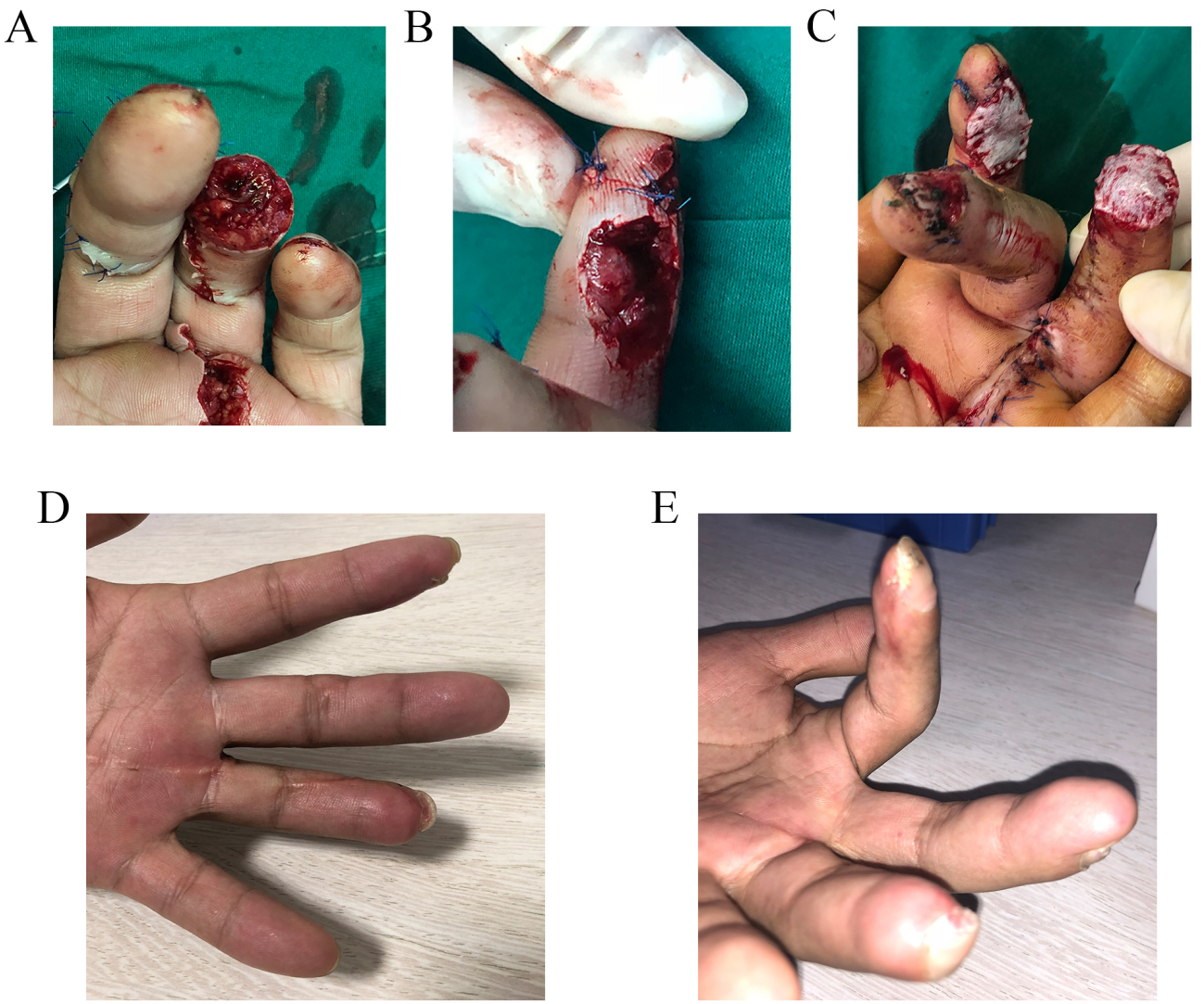

Fig. 2. Intraoperative and follow-up images of a patient with electric saw injury who received artificial dermis coverage. (A,B) DIPJ of the index finger and fingertip defect of the ring finger with underlying bone exposure. (C) Artificial dermis was covered on the wound. (D,E) The fingers healed well after operation. DIPJ, distal interphalangeal joint.

ameters range from 60 to 100 μm analysed from section view images which may be resulted from the anisotropy of the pore shape (Fig. 5D–F). Previous study has hown that the pore diameters range between those regions are optimal for cell infiltration [21]. Through the investigation of the porosity of PELNAC, we found porosity of PELNAC is 81.3 ± 2.1%. High porosity is essential for bioengineered substitutes [22,23]. The increased specific surface areas by micropores can provide more sites for protein adsorption and liquid-solid interaction to accelerate the degradation of scaffolds, which facilitate the cells growth. In addition, capillary force generated by the porosity of scaffolds can improve the attachment of cells on the scaffolds surface [24]. Liquid absorbency is an important property of wound dressing or absorbing exudates and fluid in an open wound [25]. The liquid absorbency is 1765.2 ± 56.9% examined using BS EN 13726-1: 2002, Part 1: the aspects of absorbency. The absorption capacity of PELNAC was almost equivalent to a calcium alginate dressing, which may be due to collagen component in PELNAC [26].

Degradation

Degradation property is another important characteristic of bioengineered skin substitutes as fast degradation may reduce its mechanical strength and destroy wound coverage and slow degradation will inhibit new tissue formation. To investigate the degradation behavior of PELNAC, the remaining weight of scaffolds after immersing in SBF were measured (Fig. 6). The weight of scaffolds decreased with increasing time continuously and became 86.4 ± 1.5% after a 6-week incubation, which indicated that the integrity of PELNAC could be sustained at least for 6 weeks.

Cytocompatibility

According to international standard ISO-10993-5, (Biological evaluation of medical devices Part 5: Tests for *in vitro*

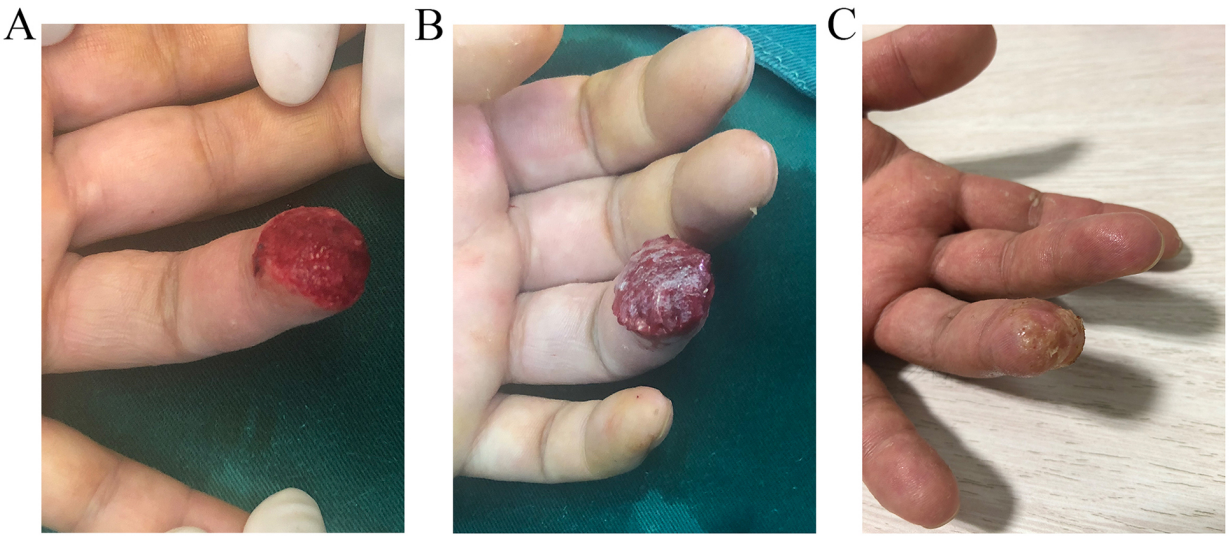

Fig. 3. Intraoperative and follow-up images of a patient with a sharp cut who received artificial dermis coverage. (A) A superficial skin and soft tissue defect of the fingertip in ring finger. (B) Artificial dermis was covered on the wound. (C) The reborn skin was similar in color and texture to normal skin.

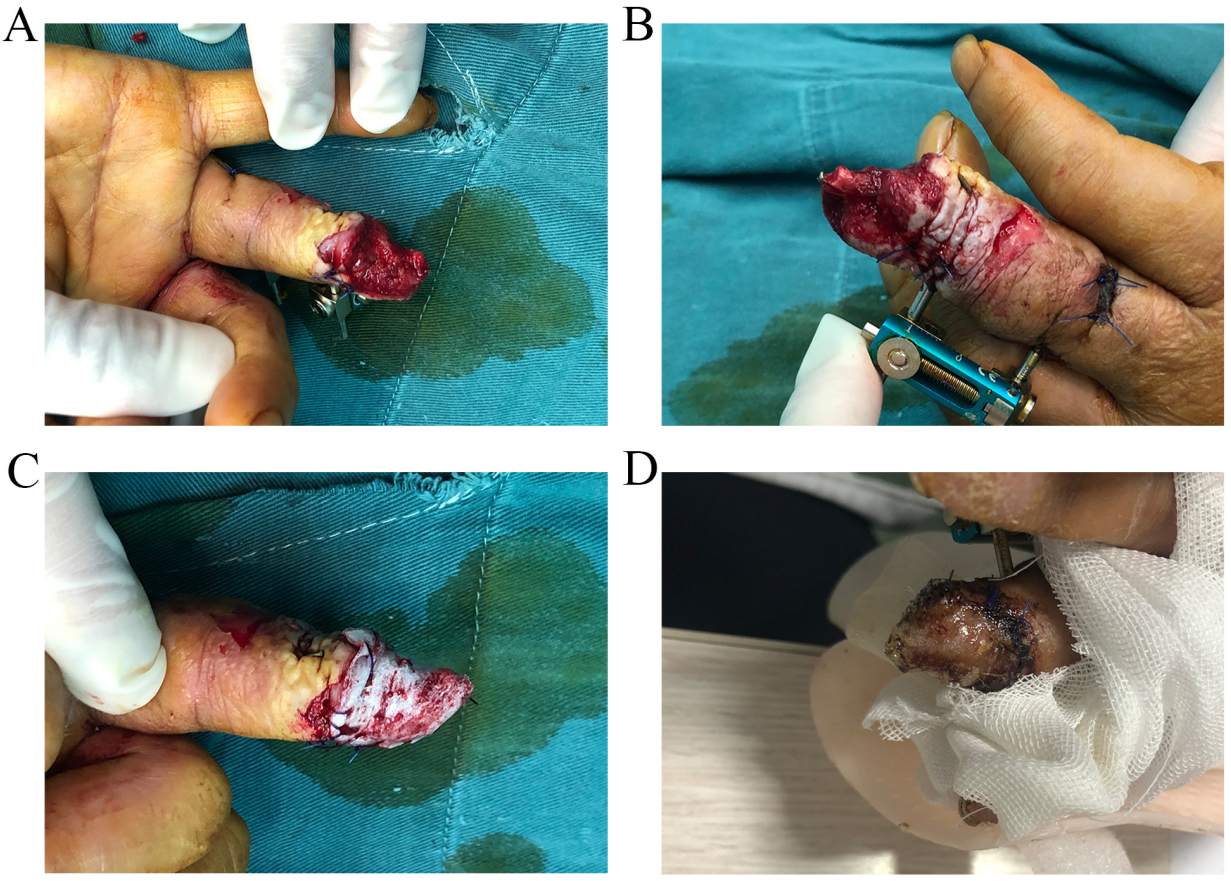

Fig. 4. Intraoperative and follow-up images of a patient with large defect of distal phalange of middle finger who received artificial dermis coverage. (A,B) A large area of deep defect in the distal phalange of ring finger with bone exposure. (C) Artificial dermis was covered on the wound. (D) The fingers healed well after operation.

cytotoxicity). L929 were selected to reveal the cytocompatibility of PELNAC. L929 cells were seeded in PELNAC and cultured for 7 days *in vitro*. SEM micrographs of the cultivated L929 in scaffolds (Fig. 7) show that cells were attached well on the surface of scaffolds and the numbers of cells increased over culture time. From the high mangnification images, which clearly indicated that there were more cells at Day 7 in scaffolds comparing those in early time

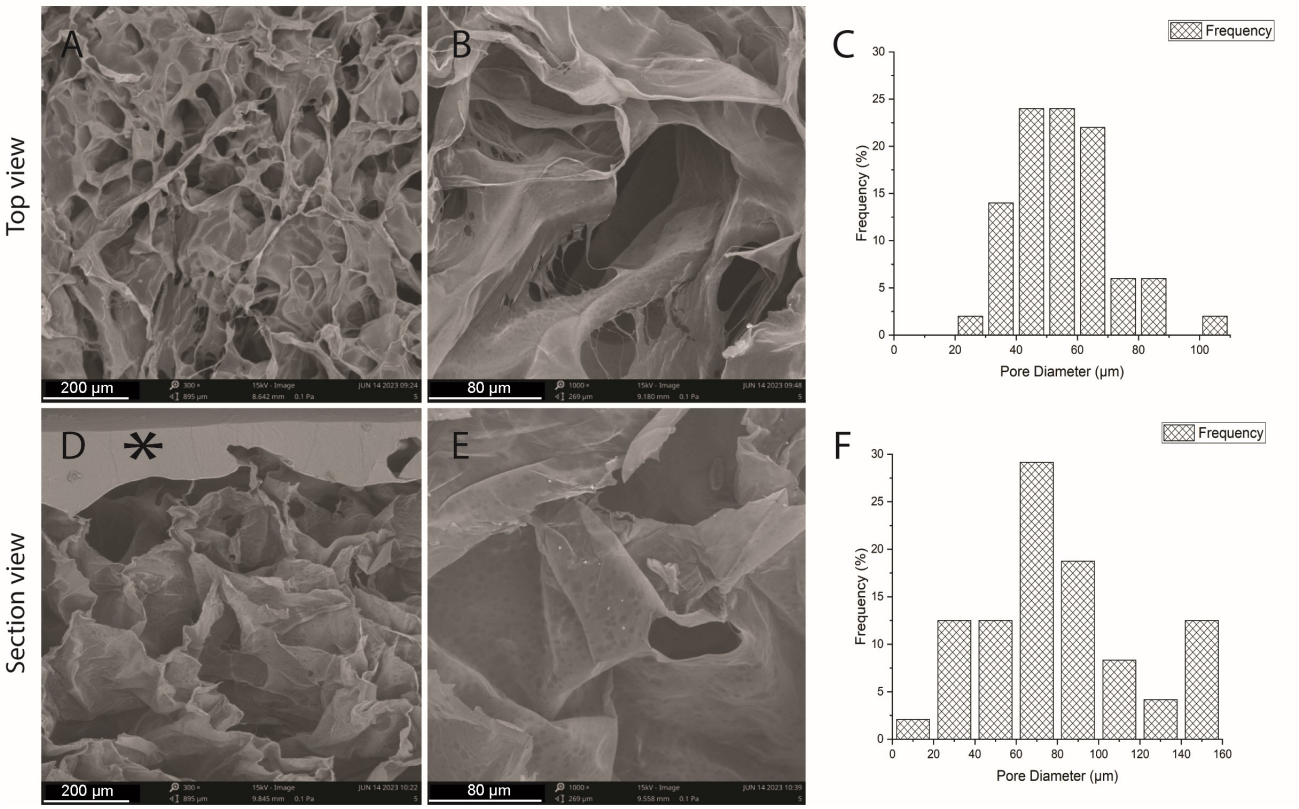

Fig. 5. The SEM images and pore diameter distributions of implantable artificial dermis-PELNAC. (A,B) are top view (collagen layer). (C) is pore diameter distribution analyzed from top view images. (D,E) are section view. (F) is pore diameter distribution analyzed from section view images. Star in section view (D) indicated silicon layer in PELNAC. SEM, Scanning electron microscope; PELNAC, Permacol Enhanced Layer for Neodermis and Coverage.

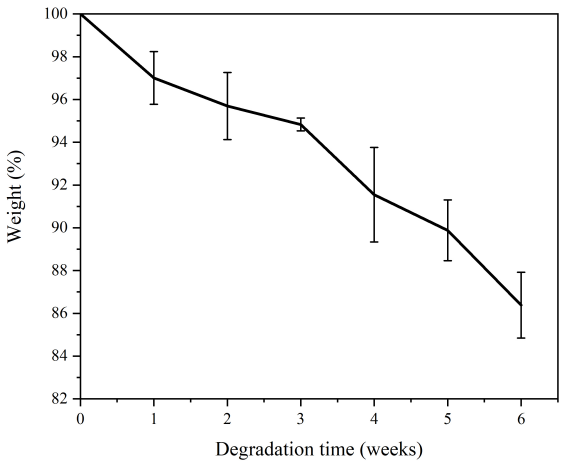

Fig. 6. *In vitro* degradation behavior of implantable artificial dermis-PELNAC in simulated body fluid (SBF) solution (pH 7.3–7.5) at 37 °C for 6 weeks.

points—Day 1 and 3. Moreover, L929 cells demonstrated round cell morphology in this PELNAC which is different from the spreading cell morphology on culture flask surfaces, which may resulted from the 3D culture envirment. These results demonstrated PELNAC possessed good cytocompatibility for cell adhesion and proliferation.

Discussion

Traumatic partial defects of the finger are common, and selecting the appropriate reconstruction method is crucial for achieving optimal outcomes. There are many surgical methods to repair finger soft tissue defects. For superficial defect, free skin transplantation is a golden standard procedure, but the transplanted skin is thin, and the appearance of the healed wound is not plump, damage to the donor site of the skin is inevitable. For deep defects, flap transplantation is necessary. V-Y advancement flaps [27], thenar pedicle flaps [28], cross-finger flaps [29], abdominal pedicle flap, reverse digital artery island flap and free flaps are considered conventional surgical methods for repairing finger soft tissue defects. The V-Y advancement flap has limited mobility and is suitable only for minor fingertip defects. High tension at the apex often leads to distal flap necrosis and impacts the function of the DIPJ. Alternatives such as cross-finger flaps, thenar flaps, and abdominal flaps require immobilization, disrupting daily activities and necessitating secondary surgeries for pedicle division. The reverse digital artery island flap compromises a digital artery, affecting finger blood supply and leaving visible lateral scars. Free flap transplantation, while an option, demands advanced microsurgical skills, carries higher risks, and often results in bulky flaps with poor aesthetic outcomes. Artificial dermis,

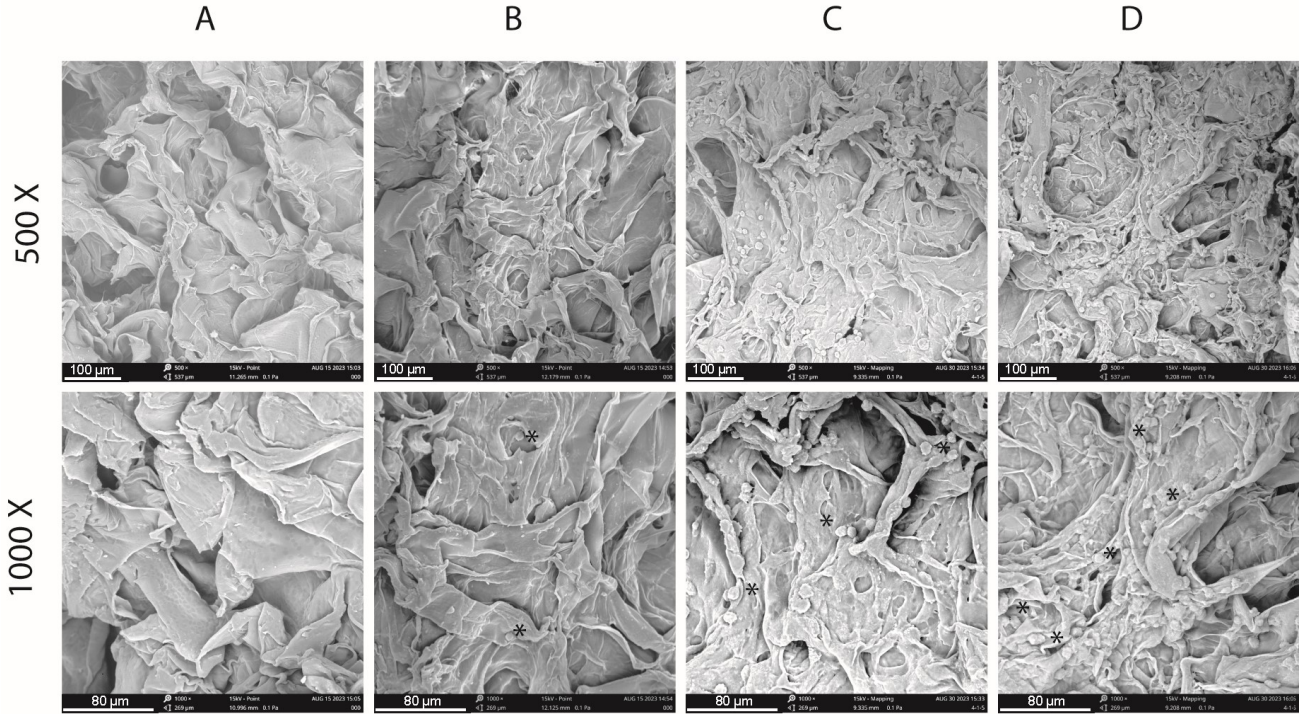

Fig. 7. The SEM images of implantable artificial dermis-PELNAC (A) and L929 cells cultured for 1 day (B); 3 days (C) and 7 days (D). Stars in (B–D) indicated cells in PELNAC.

a synthetic substitute, promotes the regeneration of dermis-like tissue and vascularization in exposed wounds, offering a promising option for reconstructive procedures. It represents an intermediate step in the reconstructive ladder between an infeasible skin graft and an avoidable flap. When applied on the wound, the dermal matrix is colonized by autologous fibroblast, creating a viable scaffold onto which split-thickness skin graft is available [30]. It permits bone, tendon, and other weakly vascularized structures to be effectively covered with vascularized tissues without the need for a flap. Various artificial dermal replacements are being created and utilized in clinical practice to cure wounds [29]. Artificial dermis grafts for finger defect reconstruction are simple to perform, with a high success rate and short operative times. They reduce the need for complex surgeries, minimize patient surgical burden, are versatile for defects of various levels and angles, provide thin, hairless skin, avoid uncomfortable immobilization, maintain finger length, minimize painful dressing changes, and are suitable for multiple fingertip amputations. It is feasible to achieve excellent sensory restoration while also reducing donor-site morbidity. It is particularly important to cover the wound at an early stage and shorten the length of stay when the medical resources are in short supply during epidemic [31,32]. But the application of artificial dermis graft is commonly used for superficial defects of the skin or soft tissue, especially when donor site of the skin is not enough and needs two steps surgeries. In contrast, other skin alternatives such as Integra (LifeSciences, Princeton, NJ, USA), while also widely used in the clinic, may not perform as well as PELNAC in some respects. Pelnac is thinner and softer than Integra, making it easier to apply to uneven wound surfaces. In terms of epidermal proliferation and skin rejuvenation, Pelnac is more restorative [9]. Integra required additional surgery to remove its silicone layer in order for a final skin graft to be performed. PELNAC showed faster healing, greater wound contraction, and better scar control in superficial wounds [9].

Artificial dermis graft PELNAC, possessed many interconnective pores and the major pore sizes ranges from 40 to 100 µm revealed from our study facilitates cell migration into the matrix, allowing the formation of a consistent and elastic neodermis [33]. PELNACTM is a double-layered skin replacement made out of a collagen scaffold underneath a silicone membrane. The underlying atelocollagen matrix layer acts as a scaffold for the ingrowth of fibroblasts, macrophages, and endothelial cells, resulting in a genuine dermis. The top silicone layer serves as a temporary barrier to limit bacterial infiltration and moisture evaporation, thereby minimizing infection [18]. Its special shape supports tissue regeneration by giving cells the perfect substrate and encouraging the proliferation of endothelium and fibroblast cells. Pelnac encourages the production of type III collagen, which gives fibroblasts a framework to adhere to and cells covered and permeated the scaffold in fibroblast-like spindles. According to histological investigations, wounds treated with PELNAC exhibited moderate levels of inflammatory cell infiltration, suggesting that PELNAC can successfully control the inflammatory response without overreacting [9]. PELNAC

may stimulate the expression of many angiogenic factors, including Angiopoietin-1 (ANGPT1), Placental Growth Factor (PGF), and Vascular Endothelial Growth Factor A (VEGFA) [34]. The development of new blood vessels and microvessels was uniformly distributed in the tissues, and Vascular Endothelial Growth Factor (VEGF) was considerably positive [9]. Furthermore, PELNAC induces a more rapid spontaneous re-epithelization of the wound [35], or a higher wounded surface contraction, as already demonstrated by Hori and colleagues [35]. PELNAC mimics endogenous dermis, reducing disabling scar contractures and improving cosmetic outcomes [36].

In conventional methods, the out-layer silicon film of PELNAC was removed in 2–3 weeks, and a subsequent split-thickness skin graft was carried out. Based on the optimal microstructure and good cytocompatibility of PELNAC, we believe that once the bioartificial dermal replacement can be integrated as neodermis, the epidermal migration might take place as well, so we did not remove the silicon film until all the skin regeneration finished. The results showed that the reborn skin region displayed morphological features similar to those of the normal skin, even in the cases with bone or tendon exposure. The sensory restoration was good, and the scar was soft and linear. All the patients were satisfied with the appearance and function of the reborn skin. ROM was not influenced in most patients, and the influence on DIPJ was small in patients who suffered from defect in the DIPJ area. The results of our study suggest that artificial dermis is a simpler and better method than conventional methods for the reconstruction of finger body defects.

PELNAC, as an artificial dermal material, has demonstrated significant advantages in the repair of partial finger defects. It eliminates the need for secondary surgeries common in traditional methods, achieving one-stage healing with a single material. This greatly simplifies the surgical process, reducing patient suffering and surgical risks. PELNAC is effective not only for superficial defects but also for deep defects, including those exposing bone or tendon. No complications such as infection, hematoma, seroma, or painful scars were observed in the study, and none of the patients experienced severe numbness and the two-point discrimination was 5.95 mm (IQR: 5.175–6.7 mm). In contrast, simple amputation will bring a significant burden to insurance. Flap surgery needs a longer time of stay, and the whole cost is not cheap. Though the cost of the artificial dermis has not been included in our medical-care system, the total cost of this surgery is not higher than other methods of surgery. The time to complete healing may be a little longer than conventional artificial dermis coverage and split-thickness skin graft, but a second surgery is not needed, and damage to the donor site of skin is avoided. The main complications which may lead to the failure of artificial dermis include infection, hematoma formation, seroma formation, and improper mobilization. So clean wound bed, proper hemostasis, and drainage are important for wound healing. Besides, strictly postoperative surveillance of the wound is necessary. Furthermore, we have done some research about repairing wounds with complete defect of the finger body. In these cases, the exposure of tendon and bone was more severe than in case 3, and we finished one-stage wound coverage through a local rotational fascia flap combined with artificial dermis. The initial effect was good, and we will discuss it in future articles.

This study has several limitations that should be addressed in future research. First, the lack of a control group (e.g., traditional flap surgery, autologous skin grafting, or other artificial dermis products) limits the ability to directly compare the efficacy of PELNAC with existing methods. Without such comparisons, it is difficult to determine whether PELNAC offers significant advantages in terms of operative time, functional recovery, scar quality, or patient satisfaction. Future studies should incorporate randomized controlled trials (RCTs) to validate its relative benefits.

The follow-up period of 12–18 months is insufficient to assess long-term outcomes, such as scar contracture, sensory function deterioration, or tissue stability after material degradation. Extending the follow-up period to 3–5 years would provide more comprehensive insights into the long-term efficacy and safety of PELNAC. Although 47 patients (56 digits) were included, the sample size remains relatively small, and the heterogeneity in injury types (e.g., cuts, crash injuries, electric saw injuries) and depths (superficial vs. deep) may affect the consistency of the results. Future studies should expand the sample size and stratify analyses based on injury types to ensure more robust conclusions.

Conclusions

Using PELNAC alone, a functional material with interconnected micropores, high porosity, and good cytocompatibility, appears to be a simple and effective clinical intervention for improving the reconstruction of partial finger defects, avoiding donor site morbidity and the need for a second surgery. Future studies should include larger sample sizes and comparative prospective trials to evaluate the long-term benefits of PELNAC.

Availability of Data and Materials

All experimental data included in this study can be obtained by contacting the corresponding author if needed.

Author Contributions

HL, HY and FW designed the study, VK, YD, HZ, AA, WS, ZS, OA, SC performed data collection, WS, WZ, MA, SE, and SA analyzed the results, HY drafted the manuscript. All authors contributed to important editorial changes in the manuscript. All authors read and approved the final manuscript. All authors have participated sufficiently in the work and agreed to be accountable for all aspects of the work.

Ethics Approval and Consent to Participate

All subjects provided informed consent from the patients or their guardians for inclusion before they participated in the study. The study was conducted in accordance with the Declaration of Helsinki, and the protocol was approved by the Ethics Committee of the First Affiliated Hospital, Zhejiang University School of Medicine (2021-107).

Acknowledgment

Not applicable.

Funding

This research received no external funding.

Conflict of Interest

Hui Lu is serving as one of the Editorial Board members of this journal. We declare that Hui Lu had no involvement in the peer review of this article and had no access to information regarding its peer review. Siyi Chen works as a Research Associate at Zhejiang Top-medical Medical Dressing Co., Ltd. Other authors have no conflicts of interest.

References

[1] Mi S, Teng Y, Liang G, Duan C, Zhang M, Jia Z, *et al*. Effectiveness of combined tissue transplantation to repair serially damaged injuries on radial side of hand. Zhongguo Xiu Fu Chong Jian Wai Ke Za Zhi = Zhongguo Xiufu Chongjian Waike Zazhi = Chinese Journal of Reparative and Reconstructive Surgery. 2021; 35: 601–604. (In Chinese) https://doi.org/10.7507/1002-1892.202012068.

[2] Hu H, Chen H, Hong J, Mao W, Tian M, Wang L, *et al*. Propeller perforator flaps from the dorsal digital artery perforator chain for repairing soft tissue defects of the finger. BMC Surgery. 2019; 19: 188. https://doi.org/10.1186/s12893-019-0649-7.

[3] Yannas IV, Burke JF, Orgill DP, Skrabut EM. Wound tissue can utilize a polymeric template to synthesize a functional extension of skin. Science (New York, N.Y.). 1982; 215: 174–176. https://doi.org/10.1126/science.7031899.

[4] Burke JF, Yannas IV, Quinby WC, Jr, Bondoc CC, Jung WK. Successful use of a physiologically acceptable artificial skin in the treatment of extensive burn injury. Annals of Surgery. 1981; 194: 413–428. https://doi.org/10.1097/00000658-198110000-00005.

[5] Hsu KF, Chiu YL, Chiao HY, Chen CY, Chang CK, Wu CJ, *et al*. Negative-pressure wound therapy combined with artificial dermis (Terudermis) followed by split-thickness skin graft might be an effective treatment option for wounds exposing tendon and bone: A retrospective observation study. Medicine. 2021; 100: e25395. https://doi.org/10.1097/MD.0000000000025395.

[6] Suzuki S, Matsuda K, Isshiki N, Tamada Y, Yoshioka K, Ikada Y. Clinical evaluation of a new bilayer "artificial skin" composed of collagen sponge and silicone layer. British Journal of Plastic Surgery. 1990; 43: 47–54. https://doi.org/10.1016/0007-1226(90)90044-z.

[7] Kamel RA, Ong JF, Eriksson E, Junker JPE, Caterson EJ. Tissue engineering of skin. Journal of the American College of Surgeons. 2013; 217: 533–555. https://doi.org/10.1016/j.jamcollsurg.2013.03.027.

[8] Fang JJ, Li PF, Wu JJ, Zhou HY, Xie LP, Lu H. Reconstruction of massive skin avulsion of the scrota and penis by combined application of dermal regeneration template (Pelnac) and split-thickness skin graft with vacuum-assisted closure: A case report. World Journal of Clinical Cases. 2019; 7: 4349–4354. https://doi.org/10.12998/wjcc.v7.i24.4349.

[9] De Francesco F, Busato A, Mannucci S, Zingaretti N, Cottone G, Amendola F, *et al*. Artificial dermal substitutes for tissue regeneration: comparison of the clinical outcomes and histological findings of two templates. The Journal of International Medical Research. 2020; 48: 300060520945508. https://doi.org/10.1177/0300060520945508.

[10] Cottone G, Amendola F, Strada C, Bagnato MC, Brambilla R, De Francesco F, *et al*. Comparison of Efficacy among Three Dermal Substitutes in the Management of Critical Lower-Limb Wounds: The Largest Biases-Reduced Single-Center Retrospective Cohort Study in Literature. Medicina (Kaunas, Lithuania). 2021; 57: 1367. https://doi.org/10.3390/medicina57121367.

[11] De Angelis B, Gentile P, Tati E, Bottini DJ, Bocchini I, Orlandi F, *et al*. One-Stage Reconstruction of Scalp after Full-Thickness Oncologic Defects Using a Dermal Regeneration Template (Integra). BioMed Research International. 2015; 2015: 698385. https://doi.org/10.1155/2015/698385.

[12] Jacoby SM, Bachoura A, Chen NC, Shin EK, Katolik LI. One-stage Integra coverage for fingertip injuries. Hand (New York, N.Y.). 2013; 8: 291–295. https://doi.org/10.1007/s11552-013-9513-x.

[13] Burd A, Wong PSY. One-stage Integra reconstruction in head and neck defects. Journal of Plastic, Reconstructive & Aesthetic Surgery: JPRAS. 2010; 63: 404–409. https://doi.org/10.1016/j.bjps.2008.11.105.

[14] Wang W, Nie W, Liu D, Du H, Zhou X, Chen L, *et al*. Macroporous nanofibrous vascular scaffold with improved biodegradability and smooth muscle cells infiltration prepared by dual phase separation technique. International Journal of Nanomedicine. 2018; 13: 7003–7018. https://doi.org/10.2147/IJN.S183463.

[15] Yue Z, Wen F, Gao S, Ang MY, Pallathadka PK, Liu L, *et al*. Preparation of three-dimensional interconnected macroporous cellulosic hydrogels for soft tissue engineering. Biomaterials. 2010; 31: 8141–8152. https://doi.org/10.1016/j.biomaterials.2010.07.059.

[16] Hasatsri S, Pitiratanaworanat A, Swangwit S, Boochakul C, Tragoonsupachai C. Comparison of the Morphological and Physical Properties of Different Absorbent Wound Dressings. Dermatology Research and Practice. 2018; 2018: 9367034. https://doi.org/10.1155/2018/9367034.

[17] Lau CS, Hassanbhai A, Wen F, Wang D, Chanchareonsook N, Goh BT, *et al*. Evaluation of decellularized tilapia skin as a tissue engineering scaffold. Journal of Tissue Engineering and Regenerative Medicine. 2019; 13: 1779–1791. https://doi.org/10.1002/term.2928.

[18] Baryza MJ, Baryza GA. The Vancouver Scar Scale: an administration tool and its interrater reliability. The Journal of Burn Care & Rehabilitation. 1995; 16: 535–538. https://doi.org/10.1097/00004630-199509000-00013.

[19] Bijur PE, Silver W, Gallagher EJ. Reliability of the visual analog scale for measurement of acute pain. Academic Emergency Medicine: Official Journal of the Society for Academic Emergency Medicine. 2001; 8: 1153–1157. https://doi.org/10.1111/j.1553-2712.2001.tb01132.x.

[20] Pei X, Ma L, Zhang B, Sun J, Sun Y, Fan Y, *et al*. Creating hierarchical porosity hydroxyapatite scaffolds with osteoinduction by three-dimensional printing and microwave sintering. Biofabrication. 2017; 9: 045008. https://doi.org/10.1088/1758-5090/aa90ed.

[21] Bružauskaitė I, Bironaitė D, Bagdonas E, Bernotienė E. Scaffolds and cells for tissue regeneration: different scaffold pore sizes-different cell effects. Cytotechnology. 2016; 68: 355–369. https://doi.org/10.1007/s10616-015-9895-4.

[22] Vyas J, Raytthatha N, Vyas P, Prajapati BG, Uttayarat P, Singh S, *et al*. Biomaterial-Based Additive Manufactured Composite/Scaffolds for Tissue Engineering and Regenerative Medicine: A Comprehensive Review. Polymers. 2025; 17: 1090. https://doi.org/10.3390/polym17081090.

[23] Xie Y, Lee K, Wang X, Yoshitomi T, Kawazoe N, Yang Y, *et al*. Interconnected collagen porous scaffolds prepared with sacrificial PLGA sponge templates for cartilage tissue engineering. Journal

of Materials Chemistry. B. 2021; 9: 8491–8500. https://doi.org/10.1039/d1tb01559a.

[24] Zhang K, Fan Y, Dunne N, Li X. Effect of microporosity on scaffolds for bone tissue engineering. Regenerative Biomaterials. 2018; 5: 115–124. https://doi.org/10.1093/rb/rby001.

[25] Dhivya S, Padma VV, Santhini E. Wound dressings - a review. BioMedicine. 2015; 5: 22. https://doi.org/10.7603/s40681-015-0022-9.

[26] Sood A, Granick MS, Tomaselli NL. Wound Dressings and Comparative Effectiveness Data. Advances in Wound Care. 2014; 3: 511–529. https://doi.org/10.1089/wound.2012.0401.

[27] Hammouda AA, El-Khatib HA, Al-Hetmi T. Extended step-advancement flap for avulsed amputated fingertip–a new technique to preserve finger length: case series. The Journal of Hand Surgery. 2011; 36: 129–134. https://doi.org/10.1016/j.jhsa.2010.10.008.

[28] Dellon AL. The proximal inset thenar flap for fingertip reconstruction. Plastic and Reconstructive Surgery. 1983; 72: 698–704. https://doi.org/10.1097/00006534-198311000-00022.

[29] Beasley RW. Local flaps for surgery of the hand. The Orthopedic Clinics of North America. 1970; 1: 219–225.

[30] Philandrianos C, Andrac-Meyer L, Mordon S, Feuerstein JM, Sabatier F, Veran J, *et al*. Comparison of five dermal substitutes in full-thickness skin wound healing in a porcine model. Burns: Journal of the International Society for Burn Injuries. 2012; 38: 820–829. https://doi.org/10.1016/j.burns.2012.02.008.

[31] Jin Q, Zhou H, Lu H. Clinical Analysis of Causes and Countermeasures of Hand Injury During the COVID-19 Outbreak and Work Resumption Period: A Retrospective Study in a Designated Hospital in China. Inquiry: a Journal of Medical Care Organization, Provision and Financing. 2021; 58: 469580211067496. https://doi.org/10.1177/00469580211067496.

[32] Sen CK. Human Wound and Its Burden: Updated 2020 Compendium of Estimates. Advances in Wound Care. 2021; 10: 281–292. https://doi.org/10.1089/wound.2021.0026.

[33] Bloemen MCT, van Leeuwen MCE, van Vucht NE, van Zuijlen PPM, Middelkoop E. Dermal substitution in acute burns and reconstructive surgery: a 12-year follow-up. Plastic and Reconstructive Surgery. 2010; 125: 1450–1459. https://doi.org/10.1097/PRS.0b013e3181d62b08.

[34] Agostinis C, Spazzapan M, Vuerich R, Balduit A, Stocco C, Mangogna A, *et al*. Differential Capability of Clinically Employed Dermal Regeneration Scaffolds to Support Vascularization for Tissue Bioengineering. Biomedicines. 2021; 9: 1458. https://doi.org/10.3390/biomedicines9101458.

[35] Hori K, Osada A, Isago T, Sakurai H. Comparison of contraction among three dermal substitutes: Morphological differences in scaffolds. Burns: Journal of the International Society for Burn Injuries. 2017; 43: 846–851. https://doi.org/10.1016/j.burns.2016.10.017.

[36] Nocini R, Lobbia G, Zatta E, Barbera G. A comparative prospective study between the outcomes of one-stage Pelnac reconstruction and full thickness skin graft on donor site healing in the radial forearm and fibula flaps. Journal of Stomatology, Oral and Maxillofacial Surgery. 2024; 125: 101949. https://doi.org/10.1016/j.jormas.2024.101949.